Chapter 19
Highly Effective Magnetic Silica-Chitosan Hybrid for Sulfate Ion Adsorption

Sukamto, Yuichi Kamiya, Bambang Rusdiarso, and Nuryono

Abstract The contamination of sulfate ions leading to corrosion is a severe problem in the aquatic environment, and adsorption is an effective method to remove this contaminant. In this study, magnetic silica-chitosan hybrids (MP@SiO_2/CPTMS/Chi) prepared by the sol-gel method have been used for adsorbing sulfate ions from an aqueous solution. The maximum adsorption capacity (Q_{max}) of the adsorbent for sulfates was 108.50 mg g^{-1} at pH 3. The MP@SiO_2/CPTMS/Chi can be easily magnetically separated (completely separated less than 5 min) from the solution after the adsorption process. High adsorption capacity and easily magnetic separation make MP@SiO_2/CPTMS/Chi a prospective candidate adsorbent for removing sulfates from wastewater.

Keywords Magnetic silica-chitosan hybrid · Sol-gel · Sulfate · Adsorption

19.1 Introduction

Sulfate is generally found in the water surface and industrial waste, including mining, printing, dyeing waste, and pharmaceuticals. Naturally, sulfates can be formed due to the chemical dissolution and oxidation of minerals containing sulfur (Fernando et al. 2018). Sulfate ions are generally considered non-toxic to humans, but sulfate ions are potentially harmful to the living organism and the environment. The presence of sulfate ions in high concentrations in water causes an imbalance in the ecosystem's sulfur cycle. Besides that, sulfate ions may accelerate the corrosion rate of building materials containing metal (Runtti et al. 2016). Therefore, it is essential to find an effective method to remove sulfate ions from water.

Sukamto · B. Rusdiarso · Nuryono (✉)
Department of Chemistry, Faculty of Mathematics and Natural Sciences, Universitas Gadjah Mada, Bulaksumur, Yogyakarta 55281, Indonesia
e-mail: nuryono_mipa@ugm.ac.id

Y. Kamiya
Faculty of Environmental Earth Science, Hokkaido University, Kita 10 Nishi 5, Sapporo 060-0810, Japan

H.-Y. Jeon (ed.), *Sustainable Development of Water and Environment*,
Environmental Science and Engineering,
https://doi.org/10.1007/978-3-030-75278-1_19

Various methods, including electrocoagulation (Omwene and Kobya 2018), ion exchange (Du et al. 2018), adsorption (Ma et al. 2019), have been used to remove sulfate ions from wastewater. Among them, adsorption is considered one of the best methods for the pollutants' removal from wastewater because of its excellent efficiency, effectiveness, and low energy demand (Xiong et al. 2011). However, adsorption method suffers from adsorbent lost after the adsorption process and cause the formation of secondary pollutant (Narita et al. 2019).

Chitosan is a biopolymer obtained from the deacetylation of chitin from crustacean (Zhang et al. 2015). The chitosan-based adsorbent has been widely used to remove pollutants in the wastewater because of its availability, biodegradable, and low impact on the environment (Zhang et al. 2018). The presence of abundant amine and hydroxyl groups on chitosan structure can be used to support its application for removing pollutants from the environment, including heavy metal and organic matters. However, chitosan has poor mechanical stability and readily dissolves under acidic conditions, leading to a decrease in adsorption capacity (Huang et al. 2017). Chitosan has been modified with various modifiers to overcome this drawback, such as silica (Kelechi et al. 2018), La(III)-bentonite (Xu et al. 2020), and calcite (Pap et al. 2020). Chitosan combined silica, known as hybrid material, shows excellent characteristics such as large surface area, high porosity, and high mechanical stability (Juan-Diaz et al. 2016).

Silica-chitosan hybrid materials can be synthesized by using a sol-gel method with the presence of a crosslinker. One of the crosslinking agents used to prepare silica-chitosan hybrid is 3-chloropropyltrimethoxysilane (CPTMS). Even though CPTMS is not the most reactive silane agent, this organosilane is one of the most widely used organosilanes for surface modification because it is easily handled, and the alcohol by products is not volatile corrosive. On the other hand, CPTMS facilitates the formation of covalent bonds between the chitosan and the silica network to enhance the chitosan's stability.

In this study, we report silica-chitosan hybrid preparation using 3-chloropropyl trymethoxysilane as the crosslinker and introducing the magnetic property to the hybrid using natural magnetic particles (MP) separated from iron sand. The materials resulted were used to remove sulfate ions from the solution. The effect of ionic strength, solution pH, adsorption time, initial concentration, and adsorbent dosage were investigated to evaluate the adsorption characteristics of sulfates. The adsorption mechanism is predicted by applying appropriate kinetics and isotherm models.

19.2 Methods

19.2.1 Materials

The iron sand sample was taken from Bugel Beach, Kulon Progo, Yogyakarta. Chitosan (>90% DD) was purchased from cv. Chemix (Yogyakarta). Sodium silicate

solution (10.6% Na_2O and 27% SiO_2), 3-chloropropyl trymetoxysilane (CPTMS), hydrochloric acid (HCl 37%), ammonium hydroxide (NH_4OH 25%) were purchased from Merck. Potassium dihydrogen phosphate ($KH_2PO_($), hydrochloric acid (HCl 0.1 mol/L), sodium hydroxide (NaOH), glacial acetic acid (CH_3COOH) were obtained from Wako Pure Chemical Industries. Ltd (Osaka, Japan).

19.2.2 Preparation of Magnetic Particles

Iron sand was dried under sun radiation for 24 h and separated from non-magnetic components with an external magnet. Dried magnetic sand was ground to pass 200 mesh in size. The magnetic particles (100 g) were washed using 250 mL distilled water with sonication for 10 min. Washing was repeated three times, and then the magnetic particles were dried in an oven at 70 °C for 24 h.

19.2.3 Synthesis of Magnetic Silica-Chitosan Hybrids (MP@SiO_2/CPTMS/Chi)

Magnetic silica-chitosan hybrids were synthesized by the sol-gel method. Magnetic particles (MP) 0.5 g and 1 mL of HCl 1 M were placed into a beaker glass. The mixture was allowed to stand for 15 min at 25 °C. MP was then separated from HCl with an external magnet. Na_2SiO_3 solution (1 mL, 3.0 mmol) and distilled water (3 mL) were mixed to the MP, and HCl (1 M) was added dropwise until pH 10. Furthermore, the obtained mixture was stirred with a mechanic stirrer for 30 min. The mixture of chitosan (2 g, 4 mmol) and CPTMS with certain volume/mmol was added to the previous mixture. The mixture was stirred with a mechanic stirrer for 5 h. After mixing, NH_4OH solution (0.5 M) was added dropwise until pH 7.0 and gel was formed. The obtained gel was aged for one night at room temperature (25 °C). The gel was then washed using distilled water and dried in an oven at 60 °C for 24 h. The analog works were carried out with various mol ratios of CPTMS to chitosan, as shown in Table 19.1.

Table 19.1 Various mol ratios of CPTMS to chitosan

CPTMS	The mol ratio of CPTMS:chitosan	Hybrid code
0.00 mL (0 mmol)	0:4	MP@SiO_2/Chi
0.18 mL (1 mmol)	1:4	MP@SiO_2/CPTMS1/Chi
0.36 mL (2 mmol)	2:4	MP@SiO_2/CPTMS2/Chi
0.54 mL (3 mmol)	3:4	MP@SiO_2/CPTMS3/Chi
0.72 mL (4 mmol)	4:4	MP@SiO_2/CPTMS4/Chi

19.2.4 Adsorption Experiment

An adsorption experiment was conducted in a batch system. Adsorbent 0.2 g was mixed with 25 mL of sulfate solutions, and the pH was adjusted at a certain value. The mixture was shaken in a shaker (VBR-36; TAITEC Co., Ltd.) for a certain time. The adsorbent was separated magnetically by applying an external magnet, and the sulfate ion concentration in the supernatant with Ion chromatography 2001. The amount of sulfate ion per gram adsorbent in the equilibrium state (q_e, mg g^{-1}) was determined using Eq. 19.1.

$$q_e = \frac{(C_o - C_e).V}{m} \tag{19.1}$$

where C_0 is the initial concentration (mg L^{-1}), and C_e is the equilibrium concentrations of sulfate ion (mg L^{-1}), V is the volume of the solution (L), and m is the mass of adsorbent (m).

Variables investigated included pH, adsorption time, initial concentration, ionic strength, and adsorbent dosage. The solution pH effect was investigated by adjusting the initial pH in the range of 2-7 using HCl (0.1 M) and NaOH (0.1 M). The effect of adsorption time was evaluated by varying contact time from 20 to 180 min. The experimental data was then analyzed using pseudo-first order (PFO) and pseudo-second-order (PSO) kinetics. The effect of initial concentration was evaluated by varying the concentration of sulfate ion 10, 30, 50, 70, and 100 mg L^{-1}, and the experimental data were analyzed with Langmuir and Freundlich models to predict the possible adsorption mechanism. NaCl concentration and adsorbent mass were varied in the range of 0-05 M and 10-100 mg, respectively, at the optimum pH and adsorption time to investigate the effect of ionic strength and adsorbent dosage,

19.3 Result and Discussion

19.3.1 Adsorption Experiments

19.3.1.1 Effect of Initial Solution pH

The initial solution pH plays an essential role in the adsorption of sulfate ions on the adsorbent surface. The pH of a solution influences the adsorption efficiency and affects the charge density on magnetic silica-chitosan hybrids' surface. The effect of pH on sulfate's adsorption into MP@SiO_2/Chi and MP@SiO_2/CPTMS1/Chi was investigated at pH ranging from 2 to 7 (Fig. 19.1). As shown in Fig. 19.1, sulfate adsorption of MP@SiO_2/Chi and MP@SiO_2/CPTMS1/Chi reached the maximum efficiency at pH 3.0 and decreased with the increasing pH value.

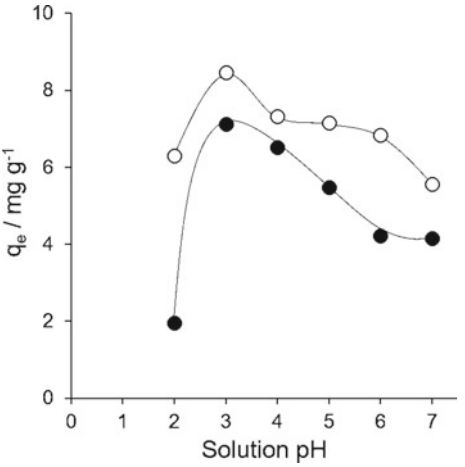

Fig. 19.1 Effect of initial pH solution on sulfate ion adsorption over (●) MP@SiO_2/Chi and (○) MP@SiO_2/CPTMS1/Chi (Conditions: sulfate ion concentration 10 mg L^{-1}; solution vol. 25 mL; adsorbent 0.02 g; temperature 30 °C; and contact time 2 h.)

The effect of the initial pH solution on the sulfate adsorption of MP@SiO_2/Chi and MP@SiO_2/CPTMS1/Chi can be explained by the point of zero charges (pH_{pzc}). The zero charge point (pH_{pzc}) for MP@SiO_2/Chi and MP@SiO_2/CPTMS1/Chi were 7.35 and 7.2, respectively (Nuryono et al. 2020). Pure silica reached the point of zero charges at pH 2, while chitosan has a positive surface charge (zeta potential) at pH lower than 6 (Anal et al. 2008). The surface of MP@SiO_2/Chi and MP@SiO_2/CPTMS1/Chi can be positively charged at pH lower than 7.35 and 7.2 due to the protonation of amine groups into ammonium groups. Therefore, the adsorption of sulfate might be attributed to the intensively electrostatic interaction between anionic sulfate species and the stable ammonium groups on the surface of materials. OH- species donate negative charge to the adsorption solution under the alkaline condition, which repulsed anionic species sulfate electrostatically. Thus, because of the electrostatic repulsion between OH^- and anionic species of sulfate, the MP@SiO_2/Chi and MP@SiO_2/CPTMS1/Chi showed low adsorption activity at pH higher than 3.

19.3.1.2 Effect of Adsorption Time and Kinetics Study

The influence of adsorption time on sulfate ion removal by MP@SiO_2/Chi and MP@SiO_2/CPTMS1/Chi can be observed in Fig. 19.2. The sulfate adsorption rate was significantly faster for the first 20 min due to an abundant active site favoring the sulfate ion adsorption. The adsorbent's active sites decreased by the increase of time and caused slower adsorption before reached equilibrium. The role of CPTMS on the structure of adsorbent also can be observed by comparing the adsorption rate between MP@SiO_2/Chi and MP@SiO_2/CPTMS1/Chi. The high density of amine groups on

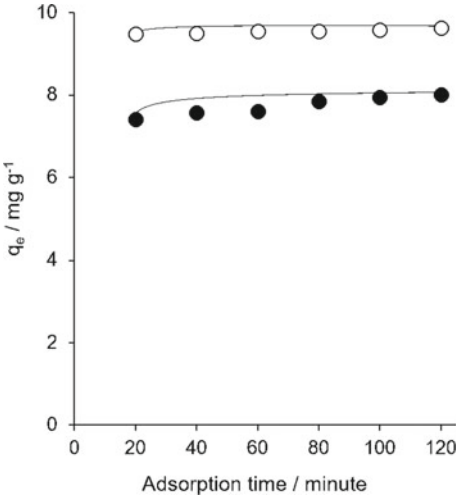

Fig. 19.2 Effect of adsorption time on the sulfate adsorption of (●) NMP@SiO_2/Chi and (○) NMP@SiO_2/CPTMS1/Chi (Conditions: sulfate ion concentration 10 mg L^{-1}; solution vol., 25 mL; adsorbent, 0.02 g; temp., 30°C; and contact time, 2 h.)

MP@SiO_2/CPTMS1/Chi promotes more vacant active sites, which increase electrostatic interaction between sulfate ion species and amine groups during adsorption time.

The sulfate adsorption mechanism was examined by applying pseudo-first-order and pseudo-second-order kinetics model to the experimental data. The pseudo-first-order kinetic model can be expressed in Eq. (19.2) as follows:

$$q_t = \mathrm{q_e} * (1 - \exp(-k_1 * t)) \tag{19.2}$$

Equation 19.2 is a nonlinear form that can be linearized in Eq. (19.3) as follows:

$$l_n(q_e - q_t) = l_n q_e - (k_{1*} t) \tag{19.3}$$

The pseudo-second-order kinetic model can be expressed in Eq. (19.4) as follows:

$$qt = (K_2 * q_{(e*)}^2 t)/(1 + (q_e * k_2 * t)) \tag{19.4}$$

Equation 4 is a nonlinear form that can be linearized in Eq. (19.5) as follows:

$$\frac{t}{q_t} = \left(\frac{1}{k_2 * q_e^2}\right) + \frac{t}{q_e} \tag{19.5}$$

$\mathrm{q_e}$ and $\mathrm{q_t}$ (mg g^{-1}) are the amounts of adsorbed sulfate ion at equilibrium, and time t, $\mathrm{k_1}$ (min^{-1}), and $\mathrm{k_2}$ (g mg^{-1} min^{-1}) is pseudo-first and second-order rate constant. The parameters obtained from pseudo-first order and pseudo-second order kinetics model for sulfate adsorption are summarized in Table 19.2.

Table 19.2 The pseudo-first and pseudo-second-order kinetic model for sulfate

Kinetics	Parameters	MP@SiO_2/Chi	MP@SiO_2/CPTMS1/Chi
Pseudo-first order	q_e^a	0.852	0.704
	k_1^b	0.014	0.063
	R^2	0.912	0.823
Pseudo-second order	q_e^c	10.225	12.106
	k_1^d	0.031	0.144
	R^2	0.9995	1

[a] q_e in mg. g^{-1} [c] q_e in mg. g^{-1}
[b] k_1 in min^{-1} [d] k_2 in mg. g^{-1}. min^{-1}

The correlation coefficient (R^2) (Table 19.2) calculated from the pseudo-first-order kinetic model shows unsuitable results between experimental and pseudo-first-order kinetic models due to the lower R^2 value. In contrast, pseudo-second-order obtained a higher R^2 value. The product exhibited that the sulfate adsorption follows PSO kinetic model. The introduction of chitosan to silica surfaces formed active layers containing hydroxyl and amine groups as active sites. The active sites, including hydroxyl and amine groups, can be easily accessed by sulfate species. Hydrogen bonding and electrostatic interaction may promote the adsorption rate of sulfate.

19.3.1.3 Effect of Initial Concentration and Isotherm Study

The adsorption profile of sulfate on MP@SiO_2/Chi, MP@SiO_2/CPTMS1/Chi, MP@SiO_2/CPTMS2/Chi, MP@SiO_2/CPTMS3/Chi, and MP@SiO_2/CPTMS4/Chi as the function of initial concentration increased significantly for the initial sulfate concentration from 10 to 70 mg L^{-1}. In contrast, the adsorption capacity increased steadily at 100 mg L^{-1} (Fig. 19.3).

The higher concentration of sulfate ions promotes the effective collision between sulfate ions and the adsorbent's active sites. The increasing of adsorption capacity demonstrates that the adsorbents have sufficient active sites which competent for accommodating a high gradient of sulfate ion. However, the materials' adsorption capacity steadily increased when the initial sulfate concentration is 100 mg L-1, which causes by the saturation of the adsorbent's active sites under a high concentration of adsorbate. The detailed investigation shows that the materials' adsorption capacity decreased by increasing CPTMS concentration on the material structure. MP@SiO2/CPTMS2/Chi achieves the highest adsorption capacity. The rise of crosslinker concentration on the magnetic silica-chitosan hybrid materials decreases the chitosan's active site due to the crosslinker's reaction with the nitrogen atom of the chitosan, which forms a denser polymer network inside the material (Osifo et al. 2008).

The mechanisms of sulfate adsorption have been investigated by applying Langmuir and Freundlich isotherm models. The maximum adsorption

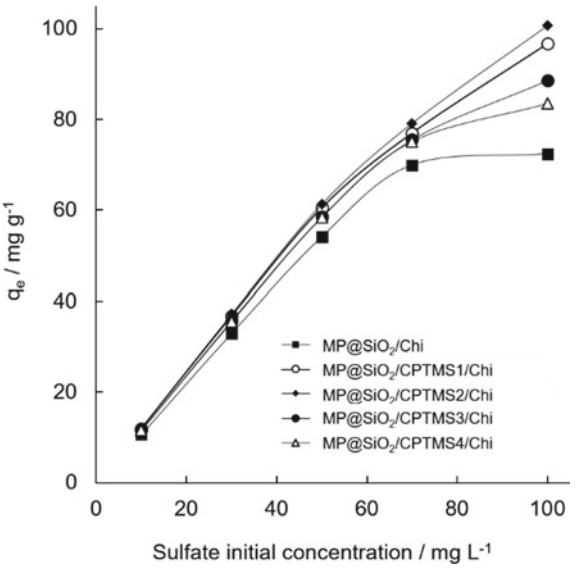

Fig. 19.3 Effect of initial sulfate concentration (Conditions: solution vol., 25 mL; adsorbent, 0.02 g; temp., 30 °C; and solution pH, 6 and 3)

capacity of MP@SiO_2/Chi, MP@SiO_2/CPTMS1/Chi, MP@SiO_2/CPTMS2/Chi, MP@SiO_2/CPTMS3/Chi, and MP@SiO_2/CPTMS4/Chi and other isotherm parameters were obtained by plotting experimental data to the isotherm models.

Langmuir model assumes the adsorption process occurred in a monolayer of the material surface where the active sites presented on the surface are identic and have equivalent energy (Naiya et al. 2009). The nonlinear Langmuir isotherm model can be expressed in Eq. (6) as follows:

$$q_e = \frac{Q_{max} K_L C_e}{1 + K_L C_e} \tag{19.6}$$

Equation 19.6 can be linearized in Eq. (19.7).

$$\frac{C_e}{q_e} = \frac{1}{bQ_{max}} + \frac{C_e}{Q_{max}} \tag{19.7}$$

Q_{max} (mg g^{-1}) is adsorbent maximum adsorption capacity, K_L (L mg^{-1}) is Langmuir isotherm constant. The value of Q_{max} and K_L can be obtained by fitting linear Langmuir isotherm or plotting C_e/q_e versus C_e.

The value of Gibbs free energy ($\Delta G°$) can be calculated by using K_L (units of liters per mole). According to the adsorbate charges characteristic, adsorbates studies can be divided into two groups: charged species and neutral species. The value of $\Delta G°$ for neutral species or adsorbate with weak charge can be calculated by using Eq. (19.8).

$$\Delta G^{O} = -RT \ln\left[K_L\left(1 mol L^{-1}\right)\right] - RT \ln K_L \tag{19.8}$$

In terms of ΔG° calculation, K_L must be changed to a dimensionless constant by multiplying the K_L value by 55.5 (mol water per liter). The proposed value of ΔG° was calculated by using Eq. (19.9) (Milonjic 2007).

$$\triangle G^{O} = RT \ln(55.5) K_L \tag{19.9}$$

According to Freundlich isotherm, the adsorbent surface has heterogeneous energy distribution of the active sites and the adsorption occurred by the multilayer formation on it. Nonlinear Freundlich isotherm model can be stated in Eq. (19.10) as follows:

$$q_e = K_F C_e^{\frac{1}{n}} \tag{19.10}$$

Equation (19.10) can be linearized in Eq. (11) as follows:

$$log q_e = log K_F + \frac{1}{n} log C_e \tag{19.11}$$

K_F (mg g^{-1}) is the Freundlich model's adsorption constant, and 1/n is the adsorption intensity. The value of K_F and 1/n can be determined with log q_e vs. log C_e plotting. The fit result of experimental data with linear Langmuir and Freundlich isotherm model can be observed in Fig. 19.4, and the obtained parameters are summarized in Table 19.3.

Sulfate adsorption on the magnetic silica-chitosan hybrid materials indicated better fitting to the Langmuir model with Q_{max} of 108.50 mg g^{-1}. The

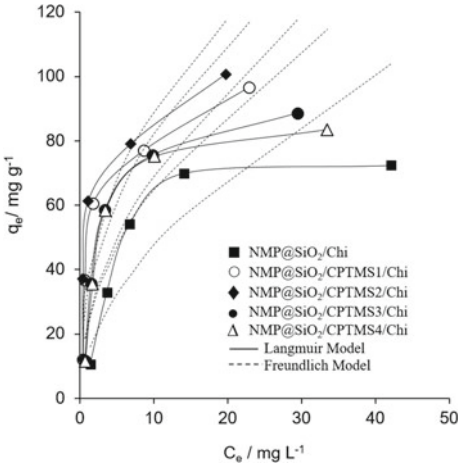

Fig. 19.4 Linear plotting of Langmuir and Freundlich isotherm model

Table 19.3 Sulfate ion adsorption parameters

Adsorbent	Langmuir			Freundlich		
	Q_{max}	K_L	R^2	n	K_F	R^2
MP@SiO_2/Chi	84.50	0.171	0.974	1.814	13.223	0.799
MP@SiO_2/CPTMS1/Chi	104.20	0.484	0.990	2.381	31.361	0.754
MP@SiO_2/CPTMS2/Chi	108.50	0.564	0.985	2.538	36.181	0.672
MP@SiO_2/CPTMS3/Chi	99.66	0.289	0.990	2.019	22.035	0.801
MP@SiO_2/CPTMS4/Chi	91.90	0.329	0.990	2.116	21.829	0.780

Table 19.4 Comparison of MP@SiO_2/CPTMS/Chi to other sulfate adsorbents

Adsorbent	Q_{max} (mg g^{-1})	References
Ni-Al	45.2	Sadeghalvad et al. (2016)
ZrBC	35.2	Ao et al. (2020)
Activated carbon from rice straw	56.49	Farahmand et al. (2015)
MP@SiO_2/CPTMS/Chi	109	Present study

MP@SiO_2/CPTMS/Chi has a higher Q_{max} than other materials, which can be summarized in Table 19.4. The comparison with other sulfate adsorbents indicated that MP@SiO2/CPTMS/Chi exhibits excellent adsorption activity toward sulfate ions.

The R_L value for sulfate ion adsorption by magnetic silica-chitosan hybrids ranged from 0.0648-0.1539. The Langmuir isotherm is conformable if the R_L lies between 0 and 1, while values higher than unity suggest an unfavorable adsorption system. Moreover, it can be confirmed by the negative $\Delta G°$ values, which shows that sulfate adsorption is spontaneous. The value of $\Delta G°$ for sulfate ion adsorption by magnetic silica-chitosan hybrid can be seen in Table 19.5. We conjecture that the silica surface was homogeneous, with the amine group as the most dominant active sites based on the Langmuir model. The proposed adsorption mechanism of sulfate by silica-chitosan hybrid materials can be shown in Fig. 19.5.

Table 19.5 Adsorption energy ($\Delta G°$) and separation factor (R_L) for sulfate adsorption

Adsorbent	K_L	$\Delta G°$	R_L
MP@SiO_2-Chi	0.1709	−5670.14	0.1539
MP@SiO_2/CPTMS1/Chi	0.4842	−8294.92	0.0648
MP@SiO_2/CPTMS2/Chi	0.5640	−8679.42	0.0565
MP@SiO_2/CPTMS3/Chi	0.2893	−6996.83	0.1011
MP@SiO_2/CPTMS4/Chi	0.3287	−7318.64	0.0908

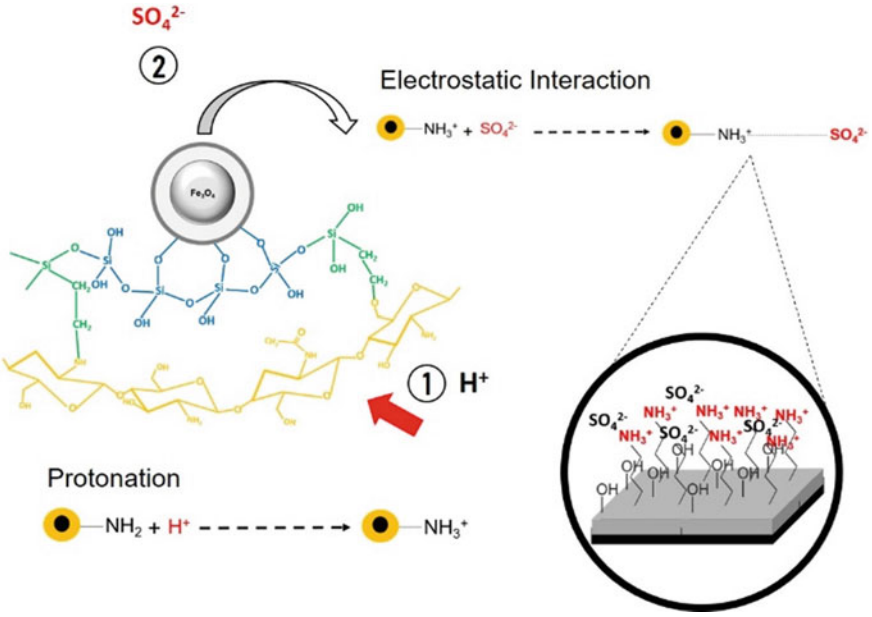

Fig. 19.5 Proposed adsorption mechanism of sulfate by silica-chitosan hybrid

19.3.1.4 Effect of Ionic Strength

The adsorption process of pollutants by an adsorbent can be caused by various interactions between adsorbate species and the adsorbent's active site. Electrostatic interaction is one of the most interactions that occurred in charged adsorbate species in the adsorption process. Most adsorption process which caused by electrostatic interaction is influenced by confounding ions. Thus, the effect of confounding ions on sulfate ion adsorption must be investigated. As shown in Fig. 19.6, the amount of adsorbed sulfate was decreased due to sodium chloride in the adsorption system. The decrease of adsorbed sulfate was caused by competitive effects between sodium ion and ammonium species on the adsorbent surface. It shows that sulfate ion adsorption by silica-chitosan hybrid materials is primarily driven by electrostatic interaction.

19.3.1.5 Effect of Adsorbent Dosage

The adsorbent dosage has a significant impact on sulfate ion adsorption. The correlation between adsorbent dosage and the adsorption capacity of the material is shown in Fig. 19.7.

The increasing of adsorbent dosage causes the increased efficiency of sulfate removal. Adsorbent dosage contributes to the increase of surface area and offers

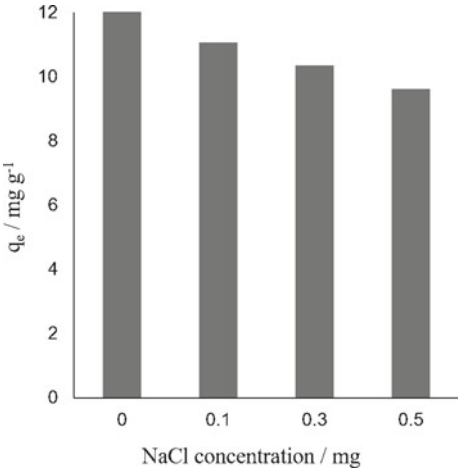

Fig. 19.6 The effect of ionic strength on sulfate adsorption (Conditions: sulfate ion concentration, 10 mg L^{-1}; solution vol., 25 mL; adsorbent, 0.02 g; temp., 30 °C; and solution pH of 3)

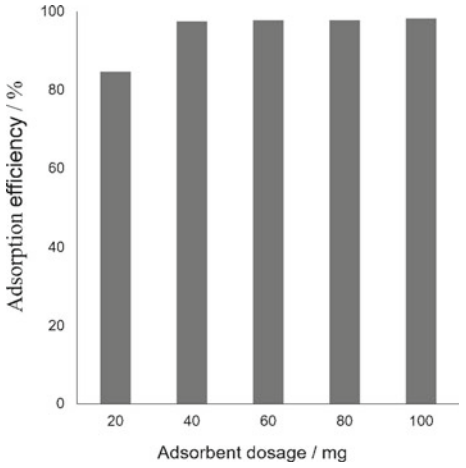

Fig. 19.7 Effect of adsorbent dosage on sulfate adsorption (Conditions: sulfate ion concentration, 10 mg L^{-1}; solution vol., 25 mL; temp., 30 °C; and solution pH of 3)

more vacant active sites, which increase the electrostatic interaction between sulfate species and active sites of the materials (Mohammadi et al. 2019).

19.4 Conclusions

In this study, the magnetic silica-chitosan hybrids synthesized from sodium silicate and chitosan using the 3-chloropropyl trimethoxysilane (CPTMS) sol-gel method were effective adsorbent for sulfate ions. The introduction of magnetic property to the silica-chitosan hybrids using natural magnetic particles produced highly magnetical separable adsorbents. It was quickly removed from the solution after the adsorption

process by applying an external magnet within less than 5 min. The effect of CPTMS addition on the adsorption showed that CPTMS at a lower concentration increased the adsorption capacity. However, at higher concentrations, the ability tended to be reduced. The mole ratio of CPTMS to chitosan 2:4 was the optimum composition to give the highest adsorption capacity of sulfate ions (108.50 mg g^{-1}). This performance makes the material produced to be prospective candidate adsorbent for removing sulfate ions from wastewater. Further research is recommended to characterize the adsorbent materials for analyzing the physical and chemical properties of materials and determine the adsorbent selectivity towards sulfate ions with various ions.

Acknowledgements The first author acknowledged the Ministry of Finance, the Republic of Indonesia for the Indonesia Endowment Fund for Education (LPDP) scholarship. This research was also financialized by the Ministry of Research and Technology/National Research and Innovation Agency through the Magister Thesis Research (PTM) Grant with the contract number: 2033/UN1/DITLIT/DIT-LIT/PT/2020.

References

Anal AK, Tobiassen A, Flanagan J, Singh H (2008) Preparation and characterizationof nanoparticles formed by chitosan–caseinate interactions. Colloids Surf B 64:104–110

Ao H, Cao W, Hong Y, Wu J, Wei L (2020) Adsorption of sulfate ion from water by zirconium oxide-modified biochar derived from pomelo peel. Sci Total Environ 708:

Du H, Lung CYK, Lau T-C (2018) Efficient adsorption, removal and recovery of phosphate and nitrate from water by a novel lanthanum(iii)-Dowex M4195 polymeric ligand exchanger. Environ Sci Technol 4:421–427

Farahmand E, Rezai B, Ardejani FD, Tonekaboni SZS (2015) Kinetics, equilibrium, and thermodynamic studies of sulfate adsorption from aqueous solution using activated carbon derived from rice straw. Bulg. Chem. Commun. 47:72–81

Fernando WAM, Ilanko IMSK, Syed TH, Yellinshetty M (2018) Challenges and opportunities in the removal of sulphate ions in contaminated mine water: a review. *Miner. Eng.* 117, 74–90

Huang R, Liu Q, Huo J, Yang B (2017) Adsorption of methyl orange onto protonated crosslinked chitosan. Arab. J. Chem. 10:24–32

Juan-Díaz MJ, Martínez-Ibánez M, Lara-Sáez I, da Silva S, Izquierdo R, Gurruchaga M, Goni I, Suay J (2016) Development of hybrid sol–gel coatings for the improvement of metallic biomaterials performance. Prog Org Coat 92:45–51

Kelechi E, Elvis OA, Kanayo AK (2018) Synthesis and Characterization of Chitosan–Silica Hybrid Aerogel using Sol-Gel Method. J. King Saud Univ. Sci. 32:550–554

Ma H, Wang M, Zhang J, Sun S (2019) Preparation mechanism of spherical amorphous $ZrO(OH)_2$/AlOOH hybrid composite beads for adsorption removal of sulfate radical from water. Mater Lett 247:56–59

Milonjic S (2007) A consideration of the correct calculation of thermodynamic parameters of adsorption. J. Serbian Chem. Soc. 72:1363–1367

Mohammadi E, Daraei H, Ghanbari R, Athar SD, Zandsalimi Y, Ziaee A, Maleki A, Yetilmezsoy K (2019) Synthesis of carboxylated chitosan modified with ferromagnetic nanoparticles for adsorptive removal of fluoride, nitrate, and phosphate anions from aqueous solutions. J Mol Liq 273:116–124

Naiya TK, Bhattacharya AK, Das SK (2009) Adsorption of Cd(II) and Pb(II) from aqueous solution on activated alumina. J Colloid Interface Sci 333:14–26

Narita Y, Sakti SCW, Akemoto Y, Tanaka S (2019) Ultra-rapid removal of cationic organic dyes by novel single- and double-stranded DNA immobilized on quaternary ammonium magnetic chitosan. J. Environ. Chem. Eng. 7:

Nuryono, Miswanda, D., Sakti, S.C.W., Rusdiarso, B., Krisbiantoro, P.A., Utami, N., Otomo, R., Kamiya, Y (2020) Chitosan-functionalized natural magnetic particle@silica modified with (3 chloropropyl)trimethoxysilane as a highly stable magnetic adsorbent for gold(III) ion, Mater. Chem. Phys., 255, 123507 (2020)

Omwene PI, Kobya M (2018) Treatment of domestic wastewater phosphate by electrocoagulation using Fe and Al electrodes: A comparative study. Process. Saf. Environ. 116:34–51

Osifo PO, Webster A, van der Merwe H, Neomagus HWJP, van der Gun MA, Grant DM (2008) The influence of the degree of crosslinking on the adsorption properties of chitosan beads. Bioresour Technol 99:7377–7382

Pap S, Kirk C, Bremner B, Sekulic MT, Shearer L, Gibb SW, Taggart MA (2020) Low-Cost Chitosan-Calcite Adsorbent Development for Potential Phosphate Removal and Recovery from Wastewater Effluent. Water Res 173:

Runtti H, Luukkonen T, Niskanen M, Tuomikoski S, Kangas T, Tynjälä P, Lassi U (2016) Sulphate removal over barium-modified blast-furnace-slag geopolymer. J Hazard Mater 317:373–384

Sadeghalvad B, Azadmehr A, Hezarkhani A (2016) Enhancing adsorptive removal of sulfate by metal layered double hydroxide functionalized Quartz-Albitophire iron ore waste: preparation, characterization and properties. RSC Adv. 6:67630–67642

Xiong J, Qin Y, Islam E, Yue M, Wang W (2011) Phosphate removal from solution using powdered freshwater mussel shells. Desalination 276:317–321

Xu X, Cheng Y, Wu X, Fan P, Song R (2020) La(III)-bentonite/chitosan composite: A new type adsorbent for rapid removal of phosphate from water bodies. Appl Clay Sci 190:

Zhang B, Chen N, Feng C, Zhang Z (2018) Adsorption for phosphate by crosslinked/non-crosslinked chitosan-Fe(III) complex sorbents: Characteristic and mechanism. Chem Eng J 353:361–372

Zhang J, Chen N, Tang Z, Yu Y, Hu Q, Feng C (2015) A study of the mechanism of fluoride adsorption from aqueous solutions onto Fe-impregnated chitosan. Phys Chem Chem Phys 17:12041–12050